ELSEVIER

CrossMark

The Spine Journal 15 (2015) 743–751

THE SPINE JOURNAL

Basic Science

Monitoring for idiopathic scoliosis curve progression using surface topography asymmetry analysis of the torso in adolescents

Amin Komeili, MSc[a,*], Lindsey Westover, MSc[b], Eric C. Parent, PT, PhD[c], Marwan El-Rich, PhD[a], Samer Adeeb, PhD[a]

[a]*Department of Civil and Environmental Engineering, University of Alberta, Markin/CNRL Natural Resources Engineering Facility, 9105 116th St, Edmonton, Alberta, Canada T6G 2W2*

[b]*Department of Mechanical Engineering, University of Alberta, 4-9 Mechanical Engineering Building, Edmonton, Canada, AB T6G 2G8*

[c]*Department of Physical Therapy, University of Alberta, 2-50 Corbett Hall, Edmonton, Alberta, Canada, T6G2G4*

Received 20 February 2014; revised 8 October 2014; accepted 8 January 2015

Abstract

BACKGROUND CONTEXT: At first visit and each clinical follow-up session, patients with adolescent idiopathic scoliosis (AIS) undergo radiographic examination, from which the Cobb angle is measured. The cumulative exposure to X-ray radiation justifies efforts in developing non-invasive methods for scoliosis monitoring.

PURPOSE: To determine the capability of the three-dimensional markerless surface topography (ST) asymmetry analysis to detect ≥5° progression in the spinal curvature in patients with AIS over 1-year follow-up interval.

STUDY DESIGN/SETTING: Cross-sectional study in a specialized scoliosis clinic.

PATIENT SAMPLE: In this study, baseline and 1-year follow-up full torso ST scans of 100 patients with AIS were analyzed using three-dimensional markerless asymmetry analysis.

OUTCOME MEASURES: Patients with ΔCobb≥5° and ΔCobb<5° were categorized into progression and nonprogression groups, respectively.

METHODS: The ST scan of each full torso was analyzed to calculate the best plane of symmetry by minimizing the distances between the torso and its reflection about the plane of symmetry. Distance between the torso and its reflection was measured and displayed as deviation color maps. The difference of ST measurements between two successive acquisitions was used to determine if the scoliosis has progressed at least 5° or not. The classification tree technique was implemented using the local deformity of the torso in the thoracic–thoracolumbar (T–TL) and lumbar (L) regions to categorize curves into progression and nonprogression groups. The change in maximum deviation and root mean square of the deviations in the torso were the parameters effective in capturing the curve progression. Funding for this research is provided by the Scoliosis Research Society, and Women and Children's Health Research Institute.

RESULTS: The classification model detected 85.7% of the progression and 71.6% of the non-progression cases. The resulting false-negative rate of 4% for T–TL curves, representing the proportion of undetected progressions, confirmed that the technique shows promise to monitor the progression of T–TL scoliosis curves. Although 100% L curves with progression were detected using the deviation color maps of the torsos, because of the small number of analyzed L curves, further research is needed before the efficiency of the method in capturing the L curves with progression is confirmed.

FDA device/drug status: Not applicable.

Author disclosures: ***AK:*** Nothing to disclose. ***LW:*** Nothing to disclose. ***ECP:*** Grant: Women and Children Health Research Institute (D); Scoliosis Research Society (C, Grant no. SFR1704). ***ME-R:*** Nothing to disclose. ***SA:*** Grant: Scoliosis Research Society (C, Grant no. SFR1704), Natural Sciences and Engineering Research Council of Canada (NSERC) (E).

The disclosure key can be found on the Table of Contents and at www.TheSpineJournalOnline.com.

* Corresponding author. 5-042, Markin/CNRL Natural Resources Engineering Facility, 9105 116th St, Edmonton, Alberta, Canada T6G 2W2. Tel.: (1) 780-200-5748.

E-mail address: akomeili@ualberta.ca (A. Komeili)

http://dx.doi.org/10.1016/j.spinee.2015.01.018

CONCLUSIONS: Using the developed classification tree for the patients analyzed in this study, 43% of nonprogression cases between two visits would not have to undergo an X-ray examination.

Keywords: Surface topography; Monitoring; Adolescent idiopathic scoliosis; Asymmetry analysis; Classification tree; Disease progression

Introduction

Scoliosis is a lateral curvature usually associated with axial rotation of the spine. The Cobb angle is the standard measurement used to quantify scoliosis severity and consists of the angle of the spine curvature between the most tilted end vertebrae of a curve on a posterior-anterior (PA) radiograph. A Cobb angle of 10° is regarded as a minimum angulation to diagnose scoliosis. Curve severity and curve progression influence treatment selection. A scoliosis curve of 10° to 20–25° is regarded as mild scoliosis and normally does not require any treatment but is monitored during regular checkups by the clinician to detect if the curve is progressive. For moderate scoliosis where the Cobb angle is 25° to 40–50°, the curve is treated nonoperatively by using a brace to prevent further curve progression. For patients with a Cobb angle that reached or exceeded 40° or 50° (severe scoliosis), correction and stabilization by orthopedic surgery is recommended [1,2]. The risk of progression is high until skeletal maturity [3–5]; therefore, frequent monitoring of adolescent idiopathic scoliosis (AIS) with any curve level is necessary. Mild curves are monitored every 6 to 9 months to detect progression and implement interventions to prevent further curve progression [6,7]. Moderate curves require monitoring to evaluate the result of bracing and because curve progression is more likely once a curve increases beyond 30° [8]. Severe curves that have not yet undergone surgery are even more likely to continue progressing over time [9].

Therefore, patients with AIS can have a radiograph every 6 months until the end of skeletal growth [10,11]. The X-ray dose and the associated lifetime risk of developing cancer is a problem justifying research on alternatives to the use of radiographs for monitoring scoliosis [12,13]. This concern is more crucial for patients with AIS compared with adult scoliosis patients because the radiation dose received is higher for younger patients [13]. Another issue with relying on radiographs is that the interpretation is sometimes difficult as radiographs represent a two-dimensional projection of the three-dimensional (3D) deformities. For instance, deformity related to spine rotation is not easily detected in standard PA radiographs.

Surface topography (ST) is a noninvasive method to investigate the 3D shape of the torso surfaces. The abnormal shape of the torso is what often convinces patients to seek consultation at a scoliosis clinic [14]. Seeking correlation between the ST indices and radiograph data motivated researchers to use ST to evaluate [15–19] and monitor the internal alignments of the spine [2,7,17,20–24]. Several studies have attempted to use ST measures to predict the magnitude of the Cobb angle or to detect changes in the Cobb angle over time with varying levels of success [2,7,25–27]. A limitation of current ST monitoring studies is the introduction of numerous ST indices, whose physical meaning may not be readily clear to the clinicians, which may contribute to the lack of agreement about the clinical value of ST methods [28,29]. Some ST studies have focused on measuring surface parameters to use as a replacement for the corresponding radiographic parameters (rotation, apex translation, and Cobb angle). To our knowledge, few ST studies have attempted to combine measurements in different surface parameters, without regard to whether these variables were conceptually equivalent to a radiograph parameter, to predict if the Cobb angle has changed. The latter may take full advantage of the surface information to minimize radiographic exposure in growing adolescents. Furthermore, an accurate and easy to implement ST technique is essential for successful noninvasive monitoring of scoliosis in patients with AIS.

In this article, we propose to analyze ST scans of patients with AIS using a 3D markerless asymmetry analysis [30]. This study aims to determine the capability of the 3D markerless ST asymmetry analysis [30] to detect $\geq 5°$ progression in the spinal curvature in patients with AIS over a 1-year follow-up interval.

Materials and methods

Subjects

Torso scans from 100 patients with AIS were selected from an ongoing study on full torso ST at the Edmonton Scoliosis Clinic. Inclusion criteria for patients in this study were a diagnosis of AIS and no surgical treatment. The first 100 consecutive patients who met the inclusion criteria and had the necessary data available were included in the study. The necessary data included a full torso ST scan with a corresponding out of brace X-ray at both a baseline time point and a follow-up time point within 12 ± 3 months from baseline. The X-ray and ST scans were taken on the same day. Approval for this study was obtained from the Health Research Ethics Board, and all subjects signed informed consent.

Four patients were excluded from the analysis because their ST asymmetry color map did not represent the

scoliosis curve in the corresponding radiograph, leaving 96 patients in the study. Also, 11 individual curves from patients with double or triple curves were excluded because the surface asymmetry map did not have an area of asymmetry associated with those curves. The excluded individual curves were 10 mild curves (eight lumbar [L] and two thoracic [T]) and one moderate curve (Table 1). All the curves that were excluded were less than 25° except one that was the smallest in a triple curve patient with curves as large as 59° (Table 1).

The final sample included 75% (n=72) females and 25% (n=24) males with Cobb angles between 10° and 69°. There were 32, 3, 13, 0, 42, and 6 subjects within the modified Lenke 1 through Lenke 6 curve types, respectively [31]. Data were collected from all consenting consecutive volunteers attending routine visits to the scoliosis clinic. Body mass index (BMI) was calculated for each patient using their weight in kilograms divided by their height squared in meters as measured during their clinical visit. The mean BMI for the patients was 21 (range, 13–34). Fifteen patients were classified as overweight, having BMI >25. Table 2 shows the number and distribution of the subjects based on the location of the curve, magnitude of the Cobb angle, and number of curves with ≥5° progression. Because some of the subjects had double or triple curves, the number of curves exceeds the number of subjects.

Surface topography

While the patient was standing looking straight ahead and with their arms elevated at the level of the shoulders in a custom positioning frame in the ST laboratory at the Edmonton Scoliosis Clinic, four Minolta laser scanners captured the 3D surface coordinates of their full torso (accuracy of scanning, 2.4 mm). The baseline and follow-up ST scans of each individual were analyzed using the 3D markerless asymmetry analysis [30]. The best plane of symmetry was calculated for the full torso by iteratively minimizing the distances between the torso and its reflection about a plane of symmetry. The gap between the torso and its reflection was color coded using the deviation analysis to visualize the area of asymmetry. A macro was developed in Mathematica (version 8.0, Wolfram Research, Chicago, IL, USA) to isolate the area of asymmetry (ie, points with |deviation| ≥±3 mm) from the deviation color map (DCM) of the whole torso to assess each scoliosis curve separately [30,32]. The back view of one analyzed torso with its corresponding radiograph is presented in Fig. 1. Visual appraisal of the 96 analyzed torsos showed that the darker the DCM the larger the Cobb angle would be (Fig. 1). Our hypothesis was that there is a direct relation between change in the asymmetry of the torso and the change in the Cobb angle (ΔCobb). The maximum deviation of the color patch (MaxDev), square root of mean squares (RMS), and area of the color patch were selected as the descriptive parameters of asymmetry:

$$\begin{aligned} \text{MaxDev} &= \text{Maximum}(\text{deviation}_i) \quad i=1,\ldots,n \\ \text{RMS} &= \sqrt{\frac{\Sigma(\text{deviation}_i^2)}{n}} \quad i=1,\ldots,n \end{aligned} \tag{1}$$

where, n is the total number of recorded points by the laser scanners. The area of the color patch was measured using Geomagic Qualify 2013 built-in commands. The change between baseline and the follow-up in the square root of mean squares (ΔRMS) of the color patch deviations, the change in the maximum deviation for each color patch (ΔMaxDev), and the percentage of change for the area (ΔA%) covered by each asymmetry color patch were calculated.

Table 1
Subjects and curves (bolded) that were excluded from the analysis because no area of asymmetry could be observed in the surface asymmetry map that corresponded to curves observed on the radiograph

				ΔCobb°		
Exclusions	Baseline curve	Follow-up curve	BMI	UT	T–TL	L
Excluded subjects	5R–UT; **10L–TL***; 8R–L	**9L–TL**; 7R–L	20		−1	−1
	17R–T; 18L–TL	21R–T	20		4	
	21R–T; 20L–TL	**15L–TL**	19		−6	
	22L–L	22R–T; **22L–L**	21			0
Excluded curves from double or triple scoliosis curve	**11R–T**; 10L–L	**11R–T**; 9L–L	15		0	−1
	15L–UT; 11R–T; **10L–L**	15L–UT; **12R–T**; 12L–TL	21	0	+1	+2
	16R–T; **13L–L**	19R–T; 17L–L	27		+3	+4
	21L–UT; 21R–T; **16L–L**	21L–UT; 18R–T; **19L–L**	20	0	−3	+3
	19R–T; **17L–L**	25R–T; 24L–L	15		+6	+7
	17R–T; 41L–TL	27R–T; 48L–TL	18		+10	+7
	26R–T; **18L–L**	22R–T; 13L–L	20		−4	−5
	24L–UT; 28R–T; **22L–L**	25L–UT; 28R–T; 16L–L	22	+1	0	−6
	38R–TL; **22L–L**	38R–TL; 28L–L	17		0	+6
	35R–T; 29L–L	21L–UT; 30R–T; **24L–L**	21		−5	−5
	46L–UT; 59R–T; **34L–L**	46L–UT; 58R–T; 37L–L	22	0	−1	+3

BMI, body mass index; R, right; L, left; UT, upper thoracic; T, thoracic; TL, thoracolumbar; L, lumbar.
* This curve did not appear in the deviation color map of torso, ΔCobb°: curve progression.

Table 2
Distribution of the curves at baseline based on the location of curve and Cobb angle value

Exclusions	Location of curve	Mild Cobb<25°	Moderate 25°≤Cobb<40°	Severe 40°≤Cobb	Total
Sample (96 subjects)	T–TL	40 (7)*	33 (4)	24 (8)	97 (19)
	L	11 (1)	10 (2)	9 (4)	30 (7)

T–TL, thoracic–thoracolumbar; L, lumbar.
* Number of curves (number of curves with ≥5° Cobb angle progression).

Radiograph analysis

A standard PA radiograph was taken for each patient during their clinical visit. The radiographs were obtained on the same day as the ST scans and in a similar position. The baseline and follow-up radiographic Cobb angle measurements corresponding to the ST scans obtained by the clinical engineer were retrieved from the clinical database to calculate the ΔCobb over the interval. All X-rays were digital, and the Cobb angle was measured with the measurement tools available in the IMPAX viewing software (AGFA Healthcare, Mortsel, Belgium) that is used clinically. The reliability of the Cobb angle measurements was not investigated in this study; however, inter-rater and intrarater reliability has been reported previously [33,34]. A mean error of 5° has been reported in Cobb angle measurement from radiographs because the end plates, from which the Cobb angle is drawn, do not have a clear trajectory as a single line on the radiograph [33]. To make sure that the change in Cobb angle exceeds measurement error, and consistent with accepted clinical practice, a change of 5° in Cobb angle was considered as the threshold to document curve progression [35,36].

Statistical analysis

The classification tree technique from SPSS, version 21, software (IBM Corp., Released 2012, Armonk, NY, USA) was used to determine the diagnostic accuracy of using thresholds in ΔRMS, ΔMaxDev, and ΔA% for detecting the progression of scoliosis. Curves with ΔCobb≥5° and ΔCobb<5° were categorized into progression and nonprogression groups, respectively.

The technique uses the selected independent variables to develop a classification tree that can be used to classify a given curve as progression or nonprogression. ΔRMS, ΔMaxDev, and ΔA% were selected as independent or predictor variables. The progression group was selected as the target variable because in a clinical setting it is more important to correctly identify the patients who have progressed than those who have not progressed. Indeed, ST should detect all cases with progression that would require further investigations and use thresholds such that clinicians can be confident that the subjects classified as nonprogression would not need immediate further investigation with a radiograph. A maximum tree depth of two was selected for the classification tree, which defines the maximum number of times that the sample will be split when making the classification.

The technique presented here was applied to each curve separately. Thus, for a patient with a double or triple curve, each curve was analyzed for progression individually. The total number of curves analyzed was 127 (97 thoracic–thoracolumbar [T–TL] and 30 L). The effect of the body mass on the ability of the asymmetry analysis of the torso to detect curve progression was studied by repeating the analysis for the subset of the sample with a BMI <25, which is the threshold for being overweight at adolescence [37]. This secondary analysis tested the hypothesis that patients with more fatty tissue may have fewer ST changes over time.

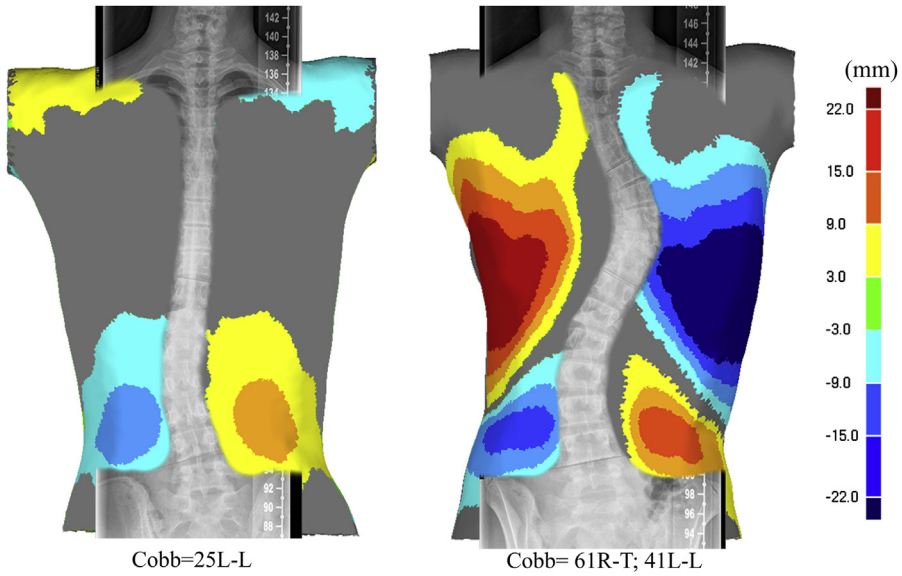

Fig. 1. Isolated color patch of two torsos with the corresponding radiograph. The Cobb angles were measured from the corresponding radiograph. L-L, Left Lumbar; R-T, Right Thoracic.

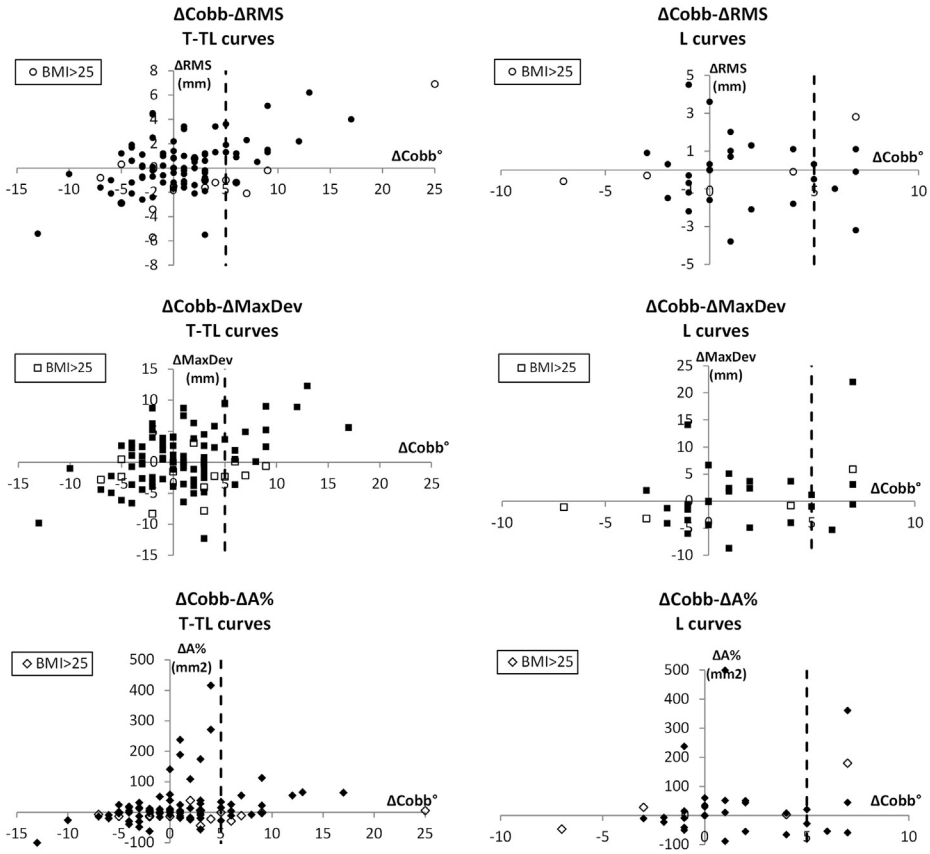

Fig. 2. Variation of square root of mean squares (ΔRMS), maximum deviation for each color patch (ΔMaxDev), and percentage of change for the area (ΔA %) versus ΔCobb for 97 thoracic–thoracolumbar (T–TL) and 30 lumbar (L) curves during 12±3 months of follow-up. Dashed line represents the boundary between progression and nonprogression based on the radiograph.

Results

A scatter plot of the association between the ΔRMS, ΔMaxDev, and ΔA% versus the ΔCobb is presented in Fig. 2 for 97 T–TL and 30 L curves with identification of the cases with BMI below and above 25. Fig. 3 shows the classification tree to classify the T–TL and L curves into progression and nonprogression groups with the accuracy of this prediction. Based on ΔCobb, it was found that 26 curves progressed (13 T–TL and 7 L) and 101 curves did not progress (78 T–TL and 23 L) over the interval of the study (Fig. 3). The ΔRMS and ΔMaxDev of the color patch were the only significant parameters to classify the T–TL curves that had progressed (ΔCobb≥5°). The ΔA% did not make a significant additional contribution to the model; therefore, it was automatically dropped. The classification tree to detect T–TL curves with progression could correctly classify 58 of 78 (specificity=74.4%) of the T–TL curves that did not progress and 13 of 19 (sensitivity=68.4%) of those that progressed. The classification tree model to detect L curves with progression correctly identified 7 of 23 (specificity=30.4%) of those that did not progress and 6 of 7 (sensitivity=85.7%) of the L curves that progressed (Fig. 3).

An analysis of the aforementioned classification results showed that most misclassified curves with progression (false negative) were for subjects with BMI≥25. There were five overweight subjects with ΔCobb≥5°, four of those were classified in nonprogression group by the first classification tree. The classification tree for subjects with BMI<25 with the number of cases for each category of each decision variable is presented in Fig. 4. Excluding the subjects with BMI≥25 from the sample led to correctly classifying a similar proportion (48 of 67, specificity=71.6%) of curves without progression and a greater proportion (12 of 14, sensitivity=85.7%) of the T–TL curves with progression. Excluding the subjects with BMI≥25 from the sample led to correctly classifying a similar proportion (7 of 20, specificity=35.0%) of L curves with no progression and an improved proportion (6 of 6, sensitivity=100%) of L curves with progression.

Discussion

In this article, change in the torso surface asymmetry of patients with AIS could help identify patients with and mostly without scoliosis progression exceeding 5° in T and L regions. The T–TL and L curves were analyzed separately. For the T–TL curves, the lateral deformation of the vertebrae in the T part is transferred to the back surface

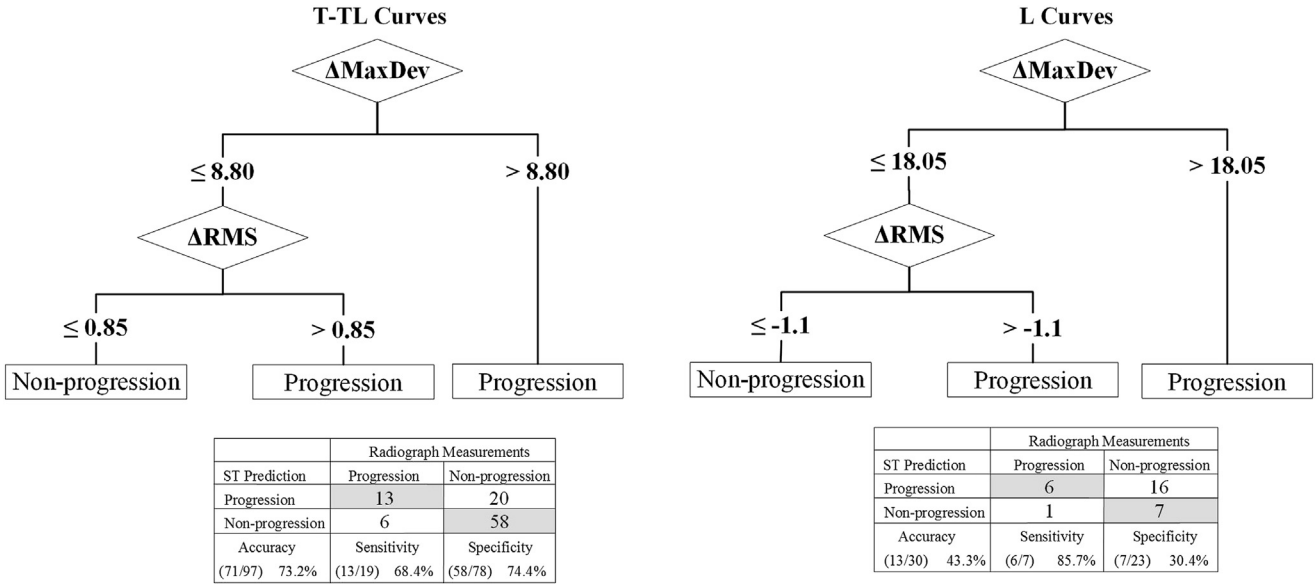

	Radiograph Measurements	
ST Prediction	Progression	Non-progression
Progression	13	20
Non-progression	6	58
Accuracy	Sensitivity	Specificity
(71/97) 73.2%	(13/19) 68.4%	(58/78) 74.4%

	Radiograph Measurements	
ST Prediction	Progression	Non-progression
Progression	6	16
Non-progression	1	7
Accuracy	Sensitivity	Specificity
(13/30) 43.3%	(6/7) 85.7%	(7/23) 30.4%

Fig. 3. Classification tree to detect curve progression ≥5° using change of root mean square (ΔRMS) and change of maximum deviation (ΔMaxDev) of the color patch for thoracic–thoracolumbar (T–TL) and lumbar (L) curves. ST, surface topography.

through the attached ribs and causes a prominent deformation on the torso surface. In contrast, the back surface in the L area is less sensitive to the vertebrae deformation because of the fact that a portion of lateral deformation in L vertebrae are damped by the surrounding soft tissue [25], which justifies our analyzing these regions separately.

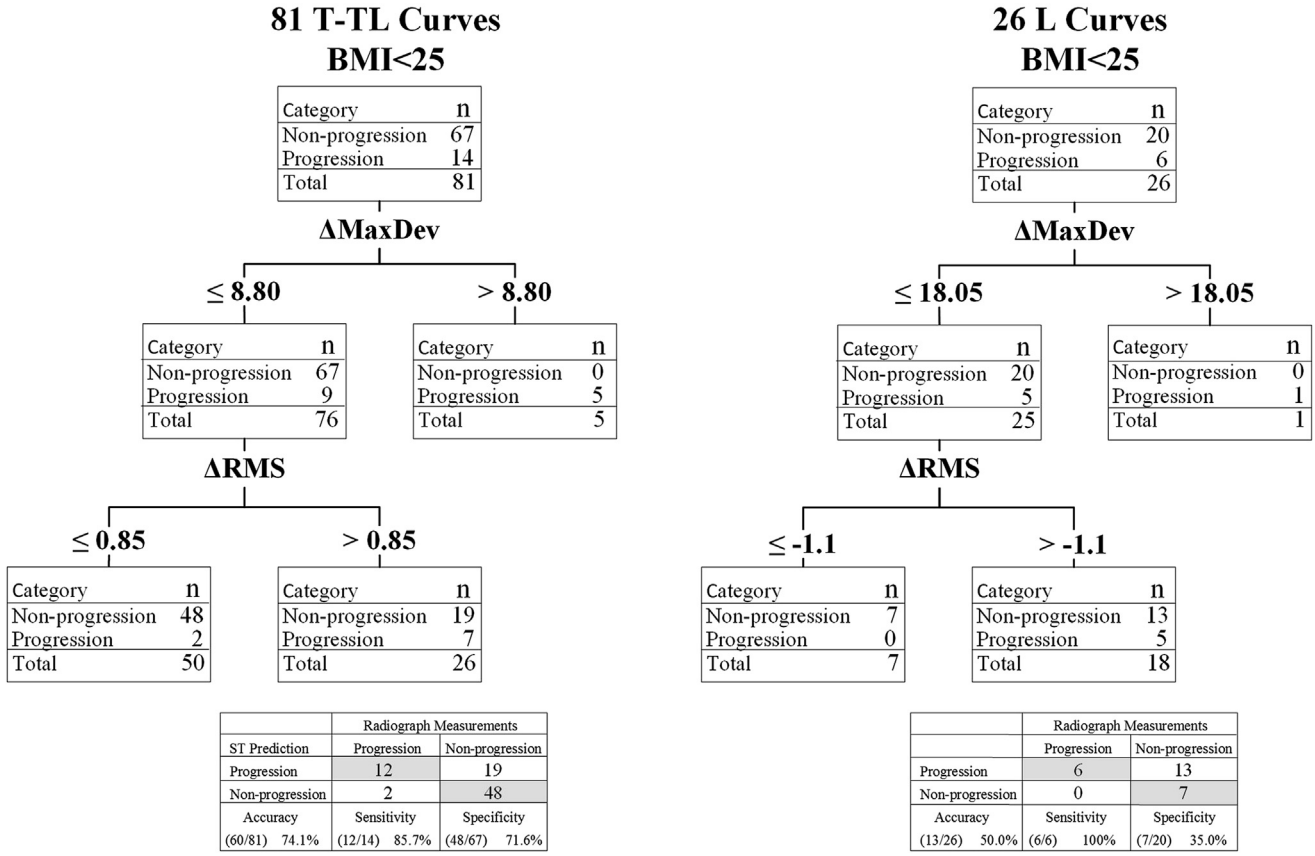

	Radiograph Measurements	
ST Prediction	Progression	Non-progression
Progression	12	19
Non-progression	2	48
Accuracy	Sensitivity	Specificity
(60/81) 74.1%	(12/14) 85.7%	(48/67) 71.6%

	Radiograph Measurements	
	Progression	Non-progression
Progression	6	13
Non-progression	0	7
Accuracy	Sensitivity	Specificity
(13/26) 50.0%	(6/6) 100%	(7/20) 35.0%

Fig. 4. Identifying the curves with progression for patient with body mass index (BMI)<25 with frequency table that shows the number of cases for each category of the dependent variable. T–TL, thoracic–thoracolumbar; L, lumbar; ΔMaxDev, change of maximum deviation; ΔRMS, change of root mean square; ST, surface topography.

Other authors also obtained heterogenous results to predict curve progression over time from ST data. Using the Quantec Spinal Imaging System, Goldberg et al. [26] extracted the Quantec angle in 59 scoliosis patients to detect a 10° Cobb angle scoliosis progression over 1 year and obtained a specificity of 45% and a promising sensitivity of 100%. The Quantec angle that reflects the coronal curvature was obtained using 12 surface landmarks. However, in routine clinical application, curve progression is usually defined as a change of 5° in the Cobb angle [4], and therefore detecting a 10° change using ST may not be clinically useful.

In contrast, Theologis et al. [2] used the Integrated Shape Imaging System (Oxford Metrics Ltd, London, UK) and found significant mean differences in only one (transverse asymmetry) of five of the investigated ST parameters between groups of patients with more or less than 5° increase in the Cobb angle after 18 months. Their sample included 78 patients. Unfortunately, sensitivity and specificity for detecting a change of at least 5° was not investigated. Schulte et al. [7] found correlations between changes in Cobb angles and changes in lateral deviation or axial rotation obtained from a raster stereography (RSG) technique in nine patients with AIS during a mean 8-year follow-up. Patients had a 61% change in the Cobb angle. In contrast with the present study, the authors did not discuss the ability of the RSG parameters to detect 5° Cobb angle progression during a shorter follow-up period consistent with the interval of consecutive monitoring visits. Surprisingly, although RSG parameters were from at least a 3-year interval in a small sample, Shulte et al. concluded that RSG parameters could reduce one radiographic examination per year during the long-term follow-up of patient with AIS. Unlike in the present study, Theologis et al. and Schulte et al. only included a single curve type of only main right T curves.

Recently, Adankon et al. [27] used independent component analysis to combine surface information from 40 points on the torso and investigated the difference between ST measurements and Cobb angles over time in 30 patients with three clinical visits. Their sample consisted of 26 progressive (Cobb increase $>5°$) and 34 nonprogressive intervals. Although their method did not illustrate scoliosis deformations as in the present study, curve progression of at least 5° was detected with a high sensitivity of 92% and promising specificity of 79%. Adapting the asymmetry analysis method presented here for use with independent component analysis method of Adankon et al. may provide further improvement in the ability to predict curve progression.

In the present study, of the three ST parameters (ΔRMS, ΔMaxDev, and ΔA%) extracted from the DCM of the torso, two (ΔRMS and ΔMaxDev) proved useful to predict patients with and without at least a 5° progression in the Cobb angle during a 12±3-month follow-up period. Investigating the results showed that there were nine subjects with ΔA% >50 and ΔCobb$<5°$ (Fig. 2). The correlation of ΔA% and ΔCobb was not significant ($R^2=0.016$), which led to the exclusion of ΔA% in the classification tree for both T–TL and L curves. One explanation could be that during the follow-up period, the torso growth of patients with AIS overcomes the effect of ΔCobb in the variation of the color patch area. In addition, the radiograph of some patients who showed noticeable increase in ΔA% but ΔCobb$<5°$ showed remarkable axial rotation in the vertebral column, which could be the reason for the increase in ΔA%. The latter observation warrants further investigation of the ability of ST parameters to detect rotation changes in patients with AIS.

The model summary table provides broad information about the specifications used to build the model and the resulting classification. Excluding the subjects with BMI≥25 led to identifying 12 of 14 (85.7%) and 6 of 6 (100%) of T–TL and L curves with progression, respectively (Fig. 4), indicating that as hypothesized the method is highly sensitive to changes. This is an advantage of the classification tree because in the clinical application it is more desirable to not miss progressive curves. The goal of ST monitoring is to achieve high confidence in detecting the cases without curve progression to prevent exposure to unnecessary additional X-rays and reduce radiation doses. Our classification tree analysis was conducted to minimize the risk of missing curves with progression by maximizing the sensitivity for detecting the curves with progression, that is, only 2 of 14 (14%) T–TL curves with progression and 0 of 6 (0%) of the L curves with progression were misclassified for subjects with BMI<25. The classification table does, however, reveal one potential limitation of the classification tree: 19 of 26 (73.1%) L curves were diagnosed as having progression; however, only 6 of 26 (23.1%) L curves had progressed, which means that the model could filter only a small number of the L curves without progression (7 of 20).

Our study demonstrated that when our classification tree predicts that a patient with BMI<25 did not have curve progression using ST data, there is a probability of more than 90% that no radiographic progression has occurred. This is clinically important and warrants a validation study to confirm if the high negative predictive value of this classification tree model can be replicated in a sample of new patients. If the negative predictive value remains as good, it may be possible to safely recommend that patients classified in the nonprogression group on the basis of their ST data may avoid a radiograph at that visit.

Overall, if a clinic decided not to use radiographs in patients identified by the classification tree as having no curve progression, the number of radiographs ordered may be reduced by as much as 43%. Indeed, when the model suggested nonprogression, 96% (48 of 50) of the T–TL curves and 100% (7 of 7) of the L curves did not have radiological progression. This prediction value is clinically important although not perfect. The model identified correctly only 48 of 81 T–TL curves with no progression during the follow-up and failed to detect only 2 of 14 curves with progression. Although 6 of 6 (100%) L curves with

progression were detected using the DCM of the torso, because of the small number of L curves analyzed, no conclusion can yet be drawn about the efficiency of the method in capturing the L curves with progression. Furthermore, only 7 of 13 L curves without progression were correctly identified as having no progression suggesting that it may be possible to further improve the model.

One limitation of the method is that approximately 25% of L mild curves in patients with double or triple scoliosis did not appear in the DCM of the torso. Investigating the DCMs of patients listed in Table 1 showed that the effect of the spine curvature on external deformities in patients with double or triple scoliosis curves, especially for mild curves, tends to balance out between the T and L regions. Nevertheless, the DCM of the torso may help avoid radiographs in patients with AIS whose DCM represents all the curves observed in a baseline radiograph.

Of the 100 patients who were analyzed, only four patients with mild curves were excluded. These patients were excluded because it was not possible to run the analysis when both measurements (baseline and follow-up) are not present. For these patients, there was a mismatch between the number of curves on the X-ray and the color patches on the DCM. The reason behind this discrepancy was either because the curves were too mild (less than or equal to 10°) to be captured on the surface or because there were other areas of torso asymmetry that overshadowed the mild spinal curvature. Including these few patients who have a discrepancy between the baseline radiograph and DCM in the group of patients requiring additional X-ray would not alter the recommendations based on our analysis.

Previous studies typically examined only the largest curve of the patient; however, this study attempted to monitor each of the curves individually. Although the largest curve is likely to have the greatest influence on the clinical decision, it is still important to monitor the secondary curves to detect potential progression of the deformity. In some cases in this study, it was found that the asymmetry associated with the smaller secondary curve is sometimes overshadowed by the major curve. In this case, a curve is present on the X-ray, but it does not have an associated color patch on the DCM. This was the reason that 11 individual curves were excluded from the analysis. Because these curves were not the major curve in each patient, the fact that the curves were not detected on the DCM would likely not have a negative effect on the clinical care of the patient or clinical decision making. To the best of our knowledge, this is the first study to attempt to monitor all the curves individually. The ability to monitor all the curves simply provides additional information to the clinicians, which can help to inform their clinical decisions. In particular, detecting changes in the secondary curves can have implications in brace treatment suggesting that brace adjustments may possibly be required.

The indices extracted from our 3D markerless asymmetry analysis have some advantages over most previous shape-based indicators [26,38–40]: they are intuitive and related to the deviation of the spine from symmetry; our proposed asymmetry analysis of the full torso preserves the information of the whole torso; the proposed asymmetry measurement method does not rely on manually placed markers and thereby eliminates the measurement variation associated with error in marker placements; not relying on marker placements also facilitates the implementation of the method in the clinic. In addition, our asymmetry analysis can be used with any ST imaging system that is able to generate a 3D model of the torso surface and is independent of the coordinate system.

Conclusion

Results from this study showed that the technique is robust and clinically relevant and can be used to monitor the progression of T, TL, and L scoliosis curves. Because the results showed that the ability of our asymmetry analysis is better in larger curves we recommended to use the DCMs of the torso for patients with at least one previous radiograph to ensure the monitoring of all curves. The effect of body fat was also found to be significant, and the method might require a different classification tree for the group of patients with higher BMI. The method could reduce 43% of radiation dose by identifying 41 of 96 patients with nonprogression in T–TL and L curves. Upper T curves were not examined in the present study.

References

[1] Ulkatan S, Neuwirth M, Bitan F, Minardi C, Kokoszka A, Deletis V. Monitoring of scoliosis surgery with epidurally recorded motor evoked potentials (D wave) revealed false results. Clin Neurophysiol 2006;117:2093–101.
[2] Theologis TN, Fairbank JC, Turner-Smith AR, Pantazopoulos T. Early detection of progression in adolescent idiopathic scoliosis by measurement of changes in back shape with the Integrated Shape Imaging System scanner. Spine 1997;22:1223–7; discussion 1228.
[3] Tan KJ, Moe MM, Vaithinathan R, Wong HK. Curve progression in idiopathic scoliosis: follow-up study to skeletal maturity. Spine 2009;34:697–700.
[4] Soucacos PN, Zacharis K, Gelalis J, Soultanis K, Kalos N, Beris A, et al. Assessment of curve progression in idiopathic scoliosis. Eur Spine J 1998;7:270–7.
[5] Lee CF, Fong DY, Cheung KM, Cheng JC, Ng BK, Lam TP, et al. A new risk classification rule for curve progression in adolescent idiopathic scoliosis. Spine J 2012;12:989–95.
[6] Van Goethem J, Van Campenhout A, van den Hauwe L, Parizel PM. Scoliosis. Neuroimaging Clin N Am 2007;17:105–15.
[7] Schulte TL, Hierholzer E, Boerke A, Lerner T, Liljenqvist U, Bullmann V, et al. Raster stereography versus radiography in the long-term follow-up of idiopathic scoliosis. J Spinal Disord Tech 2008;21:23–8.
[8] Cassella MC, Hall JE. Current treatment approaches in the nonoperative and operative management of adolescent idiopathic scoliosis. Phys Ther 1991;71:897–909.
[9] Karol LA, Johnston CE, Browne RH, Madison M. Progression of the curve in boys who have idiopathic scoliosis. J Bone Joint Surg Am 1993;75:1804–10.

[10] Greulich WW, Pyle SI. Radiographic atlas of skeletal development of the hand and wrist. Stanford, CA: Stanford University Press, 1959.
[11] Pazos V, Cheriet F, Song L, Labelle H, Dansereau J. Accuracy assessment of human trunk surface 3D reconstructions from an optical digitising system. Med Biol Eng Comput 2005;43:11–5.
[12] Oxborrow NJ. Assessing the child with scoliosis: the role of surface topography. Arch Dis Child 2000;83:453–5.
[13] Levy AR, Goldberg MS, Mayo NE, Hanley JA, Poitras B. Reducing the lifetime risk of cancer from spinal radiographs among people with adolescent idiopathic scoliosis. Spine 1996;21:1540–7; discussion 1548.
[14] Liu XC, Thometz JG, Lyon RM, Klein J. Functional classification of patients with idiopathic scoliosis assessed by the Quantec system: a discriminant functional analysis to determine patient curve magnitude. Spine 2001;26:1274–8; discussion 1279.
[15] Suzuki N, Ono T, Tezuka M, Kamiishi S. Moiré topography and back shape analysis—clinical application. In: Dansereau J, ed. International symposium on three dimensional scoliotic deformities. Stuttgart, Germany: Gustav Fisher Verlag, 1992:124–8.
[16] Komeili A, Westover L, Parent E, Moreau M, El-Rich M, Adeeb S. A novel surface topography technique to evaluate torso asymmetry in adolescent idiopathic scoliosis. Paper presented at: 13th Annual Scientific Conference of the Canadian spine society, Fairmont Tremblant, Mont-Tremblant, Quebec, February 27-March 2, 2013.
[17] Liu X, Tassone JC, Thometz JG, Paulsen LC, Lyon RM, Marquez-Barrientos C, et al. Development of a 3-dimensional back contour imaging system for monitoring scoliosis progression in children. Spine Deform 2013;1:102–7.
[18] Jaremko JL, Poncet P, Ronsky J, Harder J, Dansereau J, Labelle H, et al. Genetic algorithm-neural network estimation of Cobb angle from torso asymmetry in scoliosis. J Biomech Eng 2002;124:496–503.
[19] Jaremko JL, Poncet P, Ronsky J, Harder J, Dansereau J, Labelle H, et al. Comparison of Cobb angles measured manually, calculated from 3-D spinal reconstruction, and estimated from torso asymmetry. Comput Methods Biomech Biomed Engin 2002;5:277–81.
[20] Turner-Smith AR, Harris JD, Houghton GR, Jefferson RJ. A method for analysis of back shape in scoliosis. J Biomech 1988;21:497–509.
[21] Weisz I, Jefferson RJ, Turner-Smith AR, Houghton GR, Harris JD. ISIS scanning: a useful assessment technique in the management of scoliosis. Spine 1988;13:405–8.
[22] Lyon R, Liu X, Thometz J. Reduced need for spinal radiographs with use of a raster stereography. Paper presented at: 35th Annual Meeting of the Scoliosis Research Society. October 18–21, 2000; Australia, pp. 18–21.
[23] Weiss H, Seibel S. Can surface topography replace radiography in the management of patients with scoliosis? Hard Tissue 2013;2:19.
[24] Klos SS, Liu XC, Lyon RM, Tassone JC, Thometz JG. Reliability of a functional classification system in the monitoring of patients with idiopathic scoliosis. Spine 2007;32:1662–6.
[25] Thometz JG, Lamdan R, Liu XC, Lyon R. Relationship between Quantec measurement and Cobb angle in patients with idiopathic scoliosis. J Pediatr Orthop 2000;20:512–6.
[26] Goldberg CJ, Kaliszer M, Moore DP, Fogarty EE, Dowling FE. Surface topography, Cobb angles, and cosmetic change in scoliosis. Spine 2001;26:E55–63.
[27] Adankon MM, Chihab N, Dansereau J, Labelle H, Cheriet F. Scoliosis follow-up using noninvasive trunk surface acquisition. IEEE Trans Biomed Eng 2013;60:2262–70.
[28] Lam GC, Hill DL, Le LH, Raso JV, Lou EH. Vertebral rotation measurement: a summary and comparison of common radiographic and CT methods. Scoliosis 2008;3:16.
[29] Petit Y, Aubin C, Labelle H. Three-dimensional imaging for the surgical treatment of idiopathic scoliosis in adolescents. Can J Surg 2002;45:453–8.
[30] Komeili A, Westover L, Parent E, Moreau M, El-Rich M, Adeeb S. Surface topography asymmetry maps categorizing external deformity in scoliosis. Spine J 2014;14:973–83.
[31] Parent EC, Dang R, Hill D, Mahood J, Moreau M, Raso J, et al. Score distribution of the Scoliosis Research Society-22 questionnaire in subgroups of patients of all ages with idiopathic scoliosis. Spine 2010;35:568–77.
[32] Komeili A, Westover L, Parent E, El-Rich M, Adeeb S. Correlation between a novel surface topography asymmetry analysis and radiographic data on scoliosis curvatures. Spine Deform 2015 Jan 20. [Epub ahead of print].
[33] Gstoettner M, Sekyra K, Walochnik N, Winter P, Wachter R, Bach CM. Inter- and intraobserver reliability assessment of the Cobb angle: manual versus digital measurement tools. Eur Spine J 2007;16:1587–92.
[34] Allen S, Parent E, Khorasani M, Hill DL, Lou E, Raso JV. Validity and reliability of active shape models for the estimation of Cobb angle in patients with adolescent idiopathic scoliosis. J Digit Imaging 2008;21:208–18.
[35] Lonstein J, Carlson J. The prediction of curve progression in untreated idiopathic scoliosis during growth. J Bone Joint Surg Am 1984;66:1061–71.
[36] Brooks HL, Azen SP, Gerberg E, Brooks R, Chan L. Scoliosis: a prospective epidemiological study. J Bone Joint Surg Am 1975;57:968–72.
[37] Mohokum M, Mendoza S, Udo W, Sitter H, Paletta JR, Skwara A. Reproducibility of rasterstereography for kyphotic and lordotic angles, trunk length, and trunk inclination: a reliability study. Spine 2010;35:1353–8.
[38] Patias P, Grivas TB, Kaspiris A, Aggouris C, Drakoutos E. A review of the trunk surface metrics used as scoliosis and other deformities evaluation indices. Scoliosis 2010;5:12.
[39] Ajemba PO, Durdle NG, Raso VJ. Characterizing torso shape deformity in scoliosis using structured splines models. IEEE Trans Biomed Eng 2009;56:1652–62.
[40] Ajemba PO, Durdle NG, Hill DL, Raso VJ. A torso-imaging system to quantify the deformity associated with scoliosis. IEEE Trans Instrum Meas 2007;56:1520–6.